

## Supplemental Data

### Discovery, In Vivo Activity, and Mechanism

#### of Action of a Small-Molecule p53 Activator

Sonia Lain, Jonathan J. Hollick, Johanna Campbell, Oliver D. Staples, Maureen Higgins, Mustapha Aoubala, Anna McCarthy, Virginia Appleyard, Karen E. Murray, Lee Baker, Alastair Thompson, Joanne Mathers, Stephen J. Holland, Michael J.R. Stark, Georgia Pass, Julie Woods, David P. Lane, and Nicholas J. Westwood

#### Supplemental Experimental Procedures

##### Primary screening assay

A cell based p53-dependent reporter screen of the ChemBridge DIVERSet collection (consisting of 30,000 compounds) was conducted. T22-RGC- $\Delta$ Fos-*lacZ* murine cells expressing  $\beta$ -galactosidase under the control of a p53-dependent promoter were seeded in DMEM-10% FCS medium into 96 well plates. 80 compounds were assayed in each plate at 10  $\mu$ M. 12 of the remaining wells were left untreated (DMSO only) in order to evaluate the background  $\beta$ -galactosidase activity. 2 wells in each plate were treated with 5 ng/ml and 2 with 50 ng/ml of the established p53 activator actinomycin D. After 18 hours of treatment, medium was removed, cells were lysed in 50  $\mu$ l of 1 x Lysis buffer (Promega cat. no. E3971) for 1 hour at room temperature. 150  $\mu$ l of developer mix containing 80  $\mu$ g/ml CPRG (Roche cat no. 884308), 0.53 mM MgCl<sub>2</sub> and 24 mM  $\beta$ -mercaptoethanol were then added and optical density readings (570 nm) were made after 22 hours. Normalizing these values to the average value obtained for the reading with 5 ng/ml actinomycin D in each plate allows comparison of readings obtained for compounds assayed in different plates and on different dates. A combined collection of 610 primary hits (increasing reporter activity) and compounds that were observed to clear or damage cell monolayers was selected for titration (in triplicate at 0.01, 0.1, 1 and 10  $\mu$ M). The reason for titrating compounds that were cytotoxic at the screening concentration was that they could be potent activators of p53 at lower concentrations. 60 compounds were assayed in each plate at the appropriate concentration. 28 of the remaining wells were left untreated (DMSO only). 2 wells were treated with 5 ng/ml and 2 with 50 ng/ml of actinomycin D. 4 wells were left empty, serving as cell-free blanks. Induction of the reporter was quantified for each compound at each concentration as the activation ratio (AR), defined as [(OD treated well)-(mean OD of cell-free blank)] / [(mean OD untreated well)-(mean OD cell-free blank)]. The mean activation ratio across the replicates was calculated.

From the 610 titrated compounds, 112 gave an activation ratio of greater than or equal to 2 at their optimal concentrations. This was defined as the minimum filter on activity for further evaluation (filter 1). Of the 112 compound set, 108 were resupplied by Chembridge and re-titrated to test reproducibility of bioactivity. 83 of the resupplied compounds passed the same filter of minimum p53 induction activity (filter 2).

### **Prioritising compounds by secondary assays**

The p53 dependence of reporter activation by these 83 hits was examined in H1299 cells that lack p53. Three compounds were found to induce the RGC- $\Delta$ Fos-*lacZ* reporter in a p53-independent manner. The whole hit-set from filter 2 (83 compounds) were also evaluated by testing the relative viabilities of two cell lines, ARN8 human melanoma cells expressing wild-type p53 and normal human dermal fibroblasts (NHDF), upon treatment with compounds (10  $\mu$ M) under conditions where both cell lines were in exponential growth phase. The effect of the compounds on cell viability was monitored using MTT assays. Three compounds out of 83 showed greater toxicity towards normal cells than towards the ARN8 tumor cell line. Eliminating these compounds and setting a final, more stringent threshold of potency (at AR greater than or equal to 4 at 10  $\mu$ M or 2 at less than 10  $\mu$ M) (filter 3) gave a subset of 22 compounds for further study.

The 22 compounds in filter 3 were tested for their effects on the cell cycle by FACS in SKNSH-pCMV (expressing functional p53) cells and SKNSH-DNp53 cells (where p53 function is abolished by overexpression of a dominant negative form of p53) as described (Smart et al., 1999). Most of the compounds (e.g. JJX, see Figure S1A) were found to arrest cells in the G2/M phase of the cell cycle independently of p53 status and will be described in a separate publication. Although compounds that induce G2/M arrest are of interest for cancer treatment, these molecules increase p53 levels only after long-term treatment, suggesting that they give rise to an increase in p53 activity when cells reach a particular stage of the cell cycle (e.g. G2/M). Here we were interested in identifying compounds that increase p53 in a direct fashion. To do so, we re-screened the 108 compound set in conditions where their sensitivity to cell cycle progression is assessed. T22-RGC- $\Delta$ Fos-*lacZ* cells were seeded at 110% and 50% of the density normally used for screening and the p53 activation assay was performed at the optimal concentration for each compound. Compounds were chosen whose p53 activating effect in sparsely seeded cells was not significantly more pronounced than in over-confluent cells. Small molecules containing a three or more fused-ring moiety (potentially capable of producing DNA damage through intercalation) were de-selected from this set to leave a sub-set of 11 compounds for further study. Cell cycle analysis of SKNSH cells by FACS showed that this set of 11 molecules was not dominated by agents that arrest cells in G2/M as only 2 of them did so. Tenovin-1 was one of the 9 remaining compounds with a degree of p53-dependency with regards to its effect on cell viability and on cell cycle profile (Figure S1). Furthermore, tenovin-1 increased p53 levels in cells within a short incubation time (2 hours) (Figure 1B main text) without showing indications of genotoxicity (see Figure S4). Hence, this compound was chosen for further characterisation.

### **Target identification by a yeast genetic screen: experimental procedure**

Yeast strains heterozygous for individual gene knockouts (Euroscarf) were screened in a two-step process to identify strains that showed hypersensitivity to tenovin-6. In the first step, strains were first inoculated by pinning into 550  $\mu$ l YPAD liquid medium in a deep 96-well block (1 ml wells, Matrix), sealed with a gas-permeable membrane (AeraSeal<sup>TM</sup>, Excel Scientific) and incubated without shaking at 26 °C overnight. After resuspending the cells and diluting to  $\sim 1 \times 10^5$  cells/ml in fresh YPAD medium, duplicate 50  $\mu$ l samples of each strain were mixed with duplicate 50  $\mu$ l samples of YPAD containing tenovin-6 or 1% (v/v) DMSO (compound vehicle control) in 96-well plates and incubated for 22 h at 26 °C. Final concentrations of tenovin-6 in the assays were therefore 50, 16.7 and 5.5  $\mu$ M. Cells were resuspended

and then the OD<sub>600</sub> measured to monitor growth. The mean percent OD<sub>600</sub> at each compound concentration relative to the mean control value was recorded. Growth of most strains was completely suppressed at 50 μM tenovin-6 but was similar to the no compound control at 5.5 μM tenovin-6. At 16.7 μM compound, growth was typically ~90% of the control, but in a subset of strains was significantly lower. Since percent growth at 16.7 μM tenovin-6 varied systematically with the growth rate of individual strains, percent growth at this compound concentration was plotted against the mean OD<sub>600</sub> of the control assay so that candidate tenovin-6 hypersensitive ‘outlier’ strains could be identified (see Figure 4A).

In the second step, each of the 511 candidate hypersensitive strains identified in the first step was reassayed using a different procedure that permits relative growth rate to be estimated by an end-point assay in a manner that is independent of the initial cell concentration. Strains were grown overnight as above, diluted initially to ~ 3.3 × 10<sup>5</sup> cells per ml in fresh medium and then a further seven 0.67-fold dilutions were made. Samples of each dilution (50 μl) were mixed with either 50 μl YPAD containing 20 μM tenovin-6 or 0.5% (v/v) DMSO and incubated at 26 °C for 20 h, before resuspension and measurement of OD<sub>600</sub> as above. For each strain, OD<sub>600</sub> plus and minus compound was plotted against relative cell input (defining the lowest cell input as 1.0). By discarding points at either end of the dilution series as required to obtain a straight line (i.e. just retaining wells where growth was in exponential phase), a linear best fit line with at least 4 data points and a coefficient of correlation of at least 0.985 could be drawn whose slope related to the growth rate of (see Figure 4B). To compute a statistic for relative tenovin-6 sensitivity, the slope of the line plus compound divided by the slope of the control was calculated for each strain and then normalized between experiments by expression as a fraction of the average ratio calculated across all 96 strains assayed in each individual experiment. A ‘hypersensitivity index’ was then defined as the reciprocal of this value and is therefore 1.0 where cells show precisely average tenovin-6 sensitivity, but increases with increasing tenovin-6 sensitivity.

$$\text{Hypersensitivity index} = \frac{\left( \sum_{i=1}^n [\text{slope} + \text{drug}]_i \div [\text{slope} - \text{drug}]_i \right) \div n}{([\text{slope} + \text{drug}]_i \div [\text{slope} - \text{drug}]_i)}$$

Each strain was assayed independently on at least two occasions and the mean hypersensitivity index for each strain was calculated. After discarding unreliable data points where the standard error was more than 25% of the mean value and rounding values to one decimal place, a histogram of values was plotted for the vast majority of the strains assayed (Figure 4C). Table S3 (Supplemental Data) shows a ranked list of the top 16 hypersensitive strains corresponding to all strains shown in Figure 4C with a hypersensitivity index of 1.25 or greater.

### **Target identification by a yeast genetic screen: hit selection**

The two most hypersensitive yeast strains were heterozygous for knockouts of YOR008C-A and YDR496C respectively (Table S3). YOR008C-A is a nonessential, uncharacterized ORF identified in a screen for mutants impaired in their ability to undergo the diauxic shift that could be complemented by expression of mammalian Bcl-X<sub>L</sub> (Vander Heiden et al., 2002). The YOR008C-A knockout is synthetic lethal in combination with loss of *BUB3* (Daniel et al., 2006), which encodes a spindle checkpoint component. The significance of YOR008C-A identification as

hypersensitive to tenovin-6 is unclear and there is no obvious homologue in humans. YDR496C is *PUF6*, which is another nonessential gene encoding a *Pumilio* homology domain mRNA binding protein that is involved in polarized localization of mRNA in yeast (Aronov et al., 2007; Gu et al., 2004). The significance of identifying this gene in our screen is also unclear. However, the third most hypersensitive strain was heterozygous for YDL041W, a so-called ‘dubious ORF’ (<http://www.yeastgenome.org/>) that entirely overlaps *SIR2*, a gene encoding an NAD<sup>+</sup>-dependent protein deacetylase (Table S3). Yeast Sir2p is an enzyme whose human homologue SirT1 has already been associated with destabilization of p53 through deacetylation of lysine 382 (Luo et al., 2001; Vaziri et al., 2001), and subsequent work (see main text) has confirmed that both human SirT1 and SirT2 are inhibited by tenovin-6.

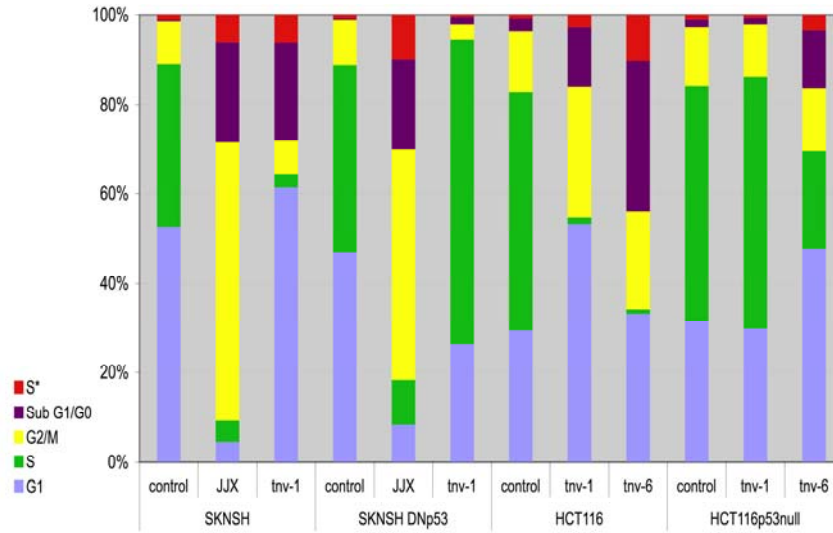
Our identification of YDL041W is surprising since the diploid strain heterozygous for a complete knockout of *SIR2* (YDL042C) did not confer hypersensitivity to tenovin-6 in the first stage of our screen, nor did it do so when checked independently using the second procedure (not shown). *SIR2* is also a nonessential yeast gene. However, the YDL041W deletion removes the region encoding the amino-terminal region of Sir2p and would potentially allow expression of a truncated version of Sir2p commencing at methionine-140 (i.e. the C-terminal 423 residues). This fragment contains the deacetylase domain but lacks much of an upstream domain that is conserved in a subset of Sir2p-related deacetylases, and may therefore act in a dominant negative manner to confer compound hypersensitivity. Furthermore, the yeast genome contains four additional genes encoding NAD<sup>+</sup>-dependent deacetylases (Brachmann et al., 1995) that may show redundancy of function. Thus while we have not explored further the basis for our identification of YDL041W in our yeast screen, we hypothesise that the Sir2p fragment expressed in this strain may confer tenovin-6 hypersensitivity by interfering with the function of multiple Sir2p family members. It is interesting to note that the heterozygous knockout of *ESC2* (YDR363W) and *ISW1* (YBR245C), encoding a Sir2p interacting proteins are also hypersensitive to tenovin-6 (see Table S3).

Another potentially interesting hit from the yeast screen was *URA8* (YJR103W), which encodes a minor CTP synthase (Table S3). CTP depletion has been shown to cause p53-dependent G1 arrest, however there is no published data showing that lowering CTP in cells leads to an increase in p53. The only evidence to date comes from the use of PALA, which inhibits synthesis of CTP and GTP. PALA increases p53 levels, but only after over 12 hours of treatment (Linke et al., 1996). Since tenovins increase p53 levels after only a 2 hour incubation, it is unlikely that inhibition of CTP synthesis is important for the effect of tenovins on p53. Long-term ribonucleotide depletion will inevitably lead to DNA damage. The fact that tenovins have no effect on comet assays performed with HaCaT cells (p53 mutant) incubated with tenovins for 24 hours (see Figure S4), further supports the notion that CTP synthesis inhibition is not an important tenovin target.

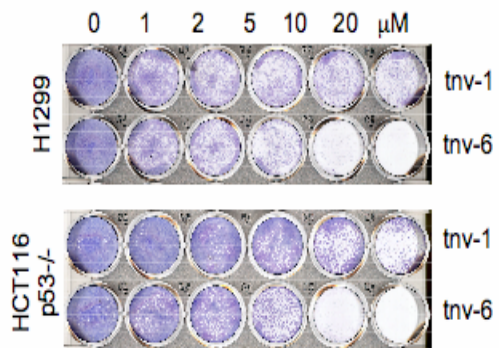
Supplemental Figures

**A**

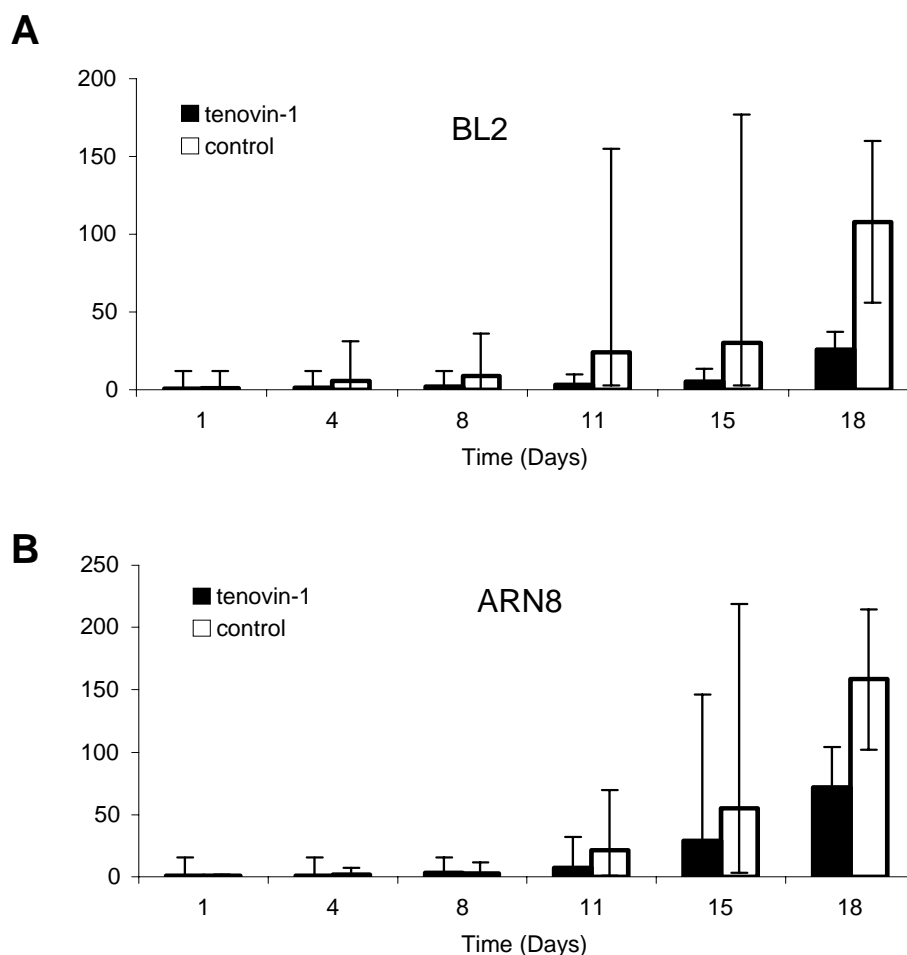
%



**B**

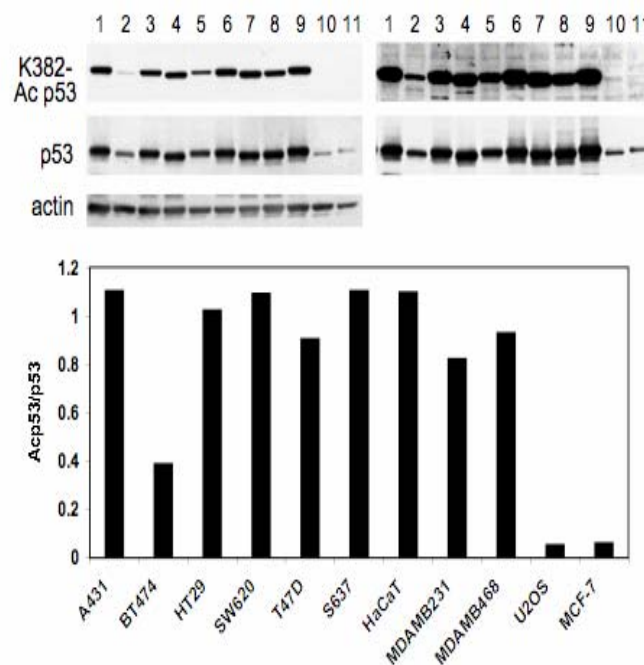


**Figure S1.** (A) Cell cycle analysis of tumor cell lines with active and inactive p53 in response to tenovins and compound JJX. Cell lines were treated with DMSO vehicle control or the indicated compound at 10  $\mu$ M for 48 hours. Cells were pulse labelled with BrdU and analysed by FACS as described (Smart et al., 1999). The percentage of cells in each stage of the cell cycle was calculated. S\* indicates cells with a DNA content between 2N and 4N but unable to incorporate BrdU. SKNSH neuroblastoma cells contain either a control vector and hence have active p53 (SKNSH-pCMV) or a vector expressing a dominant negative form of p53 (SKNSH DNp53) (Smart et al., 1999). (B) H1299 or HCT116 p53 null cells were treated with tenovin-1 for 4 days. Cells were fixed and stained with Giemsa.



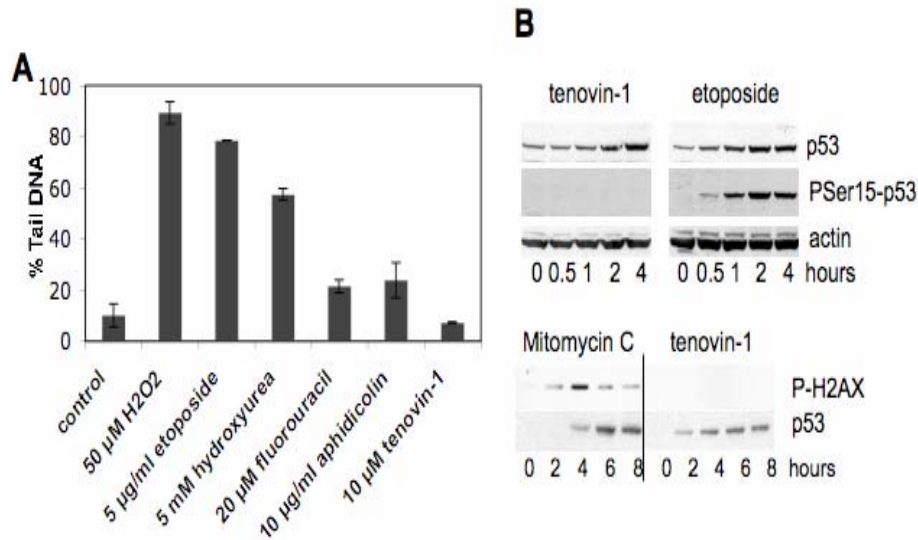
**Figure S2.** Tenovin-1 shows indications of anti-tumor activity *in vivo*. ARN8 melanoma (A) or BL2 Burkitt's lymphoma cells (B) were injected into the flank of SCID mice and allowed to develop until tumors became palpable. Tenovin-1 (in 70% cyclodextrin) was administered daily (14 days) by intraperitoneal injection at 92.5 mg/kg and tumor growth was measured over a period of 18 days. Note that mice were left untreated from day 15 to day 18. Control animals were treated with 70% cyclodextrin. In the BL2 experiment, n = 12 for each treatment. In the ARN8 experiment, n = 14 for the control group and n = 16 for the tenovin-1 treated group. Growth measurements were averaged between groups and plotted. Outliers were not

excluded. Error bars correspond to 95% confidence intervals. Mice receiving tenovin-1 had significantly reduced tumor growth as analysed by appropriate choice of 2-sample t-test (normal distributions) and Mann Whitney U-test (non-normal distributions). Difference between the tenovin-1 and control distributions were statistically significant on days 4 to 18 for BL2 tumors ( $p=0.049, 0.007, 0.000, 0.001$  and  $0.009$ , respectively) and on days 4, 11, 15 and 18 for ARN8 tumors ( $p=0.0016, 0.0133, 0.045$  and  $0.019$ , respectively). The error bars in these experiments (for both untreated and treated tumors) are larger than the ones in the experiment described in Figure 2D (main text) because in the latter experiment measurements commenced only after the tumors were better established and reached a size of approximately  $10 \text{ mm}^3$ .



**Figure S3.** Relative levels of K382-acetylated p53 in different cell lines. Equivalent amounts of protein were separated on gels and analysed with the antibody against K382-Ac p53 or DO1. Actin was analysed as a loading control. Lanes 1 through 9 correspond to cell lines expressing mutant p53 (A431, BT474, HT29, SW620, T47D, 5637, HaCaT, MDAMB231 and MDAMB468). A description of the p53 mutations in these cells can be found in <http://www-p53.iarc.fr/P53main.html>. Lanes 10 and 11 correspond to cell lines expressing wild type p53 (U2OS and MCF7). The histogram shows the ratio between the K382-Ac p53 and the DO1 signals in the left panels. Note that these values do not correspond to the actual proportion of acetylated p53 in each

cell line. The right panels show a longer exposure of the blots indicating that the Acp53/p53 ratio in U2OS cells is slightly higher than depicted in the histogram. Interestingly, BT474 encodes a thermo-sensitive mutant form of p53. This is likely to explain the intermediate Acp53/p53 value in BT474 cells.

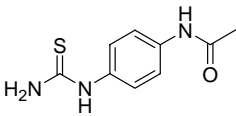
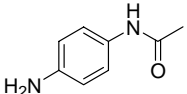
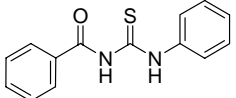
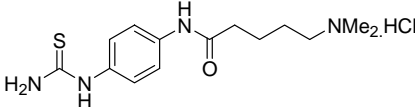


**Figure S4.** Tenovins do not cause significant DNA damage. (A) HaCaT cells were left untreated or treated with 50  $\mu\text{M}$  H<sub>2</sub>O<sub>2</sub> for 5 min at 4 °C or with the indicated DNA damaging agents or tenovin-1 for 24 hours. Comet assays were performed as described (Berkson et al., 2005). Error bars correspond to standard deviation values. (B) MCF-7 cells were treated with 10  $\mu\text{M}$  tenovin-1, 10  $\mu\text{M}$  etoposide or 20  $\mu\text{M}$  mitomycin C for the times indicated. Total p53, p53 phosphorylated at serine-15 (Cell Signaling Cat. No. 9284) or phospho-H2AX (Upstate, Cat No. 05-636) were detected. Detection of actin was used as a loading control.



## Supplemental Tables

**Table S1.** Inactive tenovin derivatives

ID	Structure	p53 increase <sup>a</sup>	K40Ac $\alpha$ -tubulin increase <sup>b</sup>	Sirt2 inhibition <sup>c</sup>
JH118		-	-	-
4-AA		-	-	-
5406085		-	-	-
AM158		-	-	-

<sup>a</sup> Ability to increase p53 levels was determined in MCF-7 cells treated for 6 hours with each compound at 10  $\mu$ M as described in Figure 1B; <sup>b</sup> Ability to increase AcK40- $\alpha$  tubulin levels was determined in H1299 cells treated as described in Figure 7B; <sup>c</sup> Sirt2 inhibition using the AK-556 kit (Biomol) as described in Table 1.

**Table S2.** Tenovin-1 and -6 pharmacokinetic parameters

<b>Parameter</b>	<b>Tnv-1, i.p. 5 mg/kg</b>	<b>Tnv-6, i.p. 10 mg/kg</b>
<b>T1/2 (h)</b>	1.0 ± 0.4	1.3 ± 0.1
<b>Cmax (ng/ml)</b>	249 ± 80 (0.67 µM)	1071 ± 214 (2.18 µM)
<b>AUC (h.ng/ml)</b>	342 ± 26	1643 ± 99
<b>CL (ml/h)</b>	388 ± 30	209 ± 12

General methodology was described in (Pass et al., 2005). Three mice were administered a tenovin-1 suspension (0.5 mg/ml in 5% DMSO) or a tenovin-6 solution (1 mg/ml in 2% DMSO) by i.p. injection (dosing volume of 10 ml/kg). Blood (10 µl) was collected directly from the tail vein at 10, 20, 30, 45, 60, 90, 120, 240 and 360 minutes, placed into a 0.5 ml tube containing 10 µl water and then snap frozen in liquid N<sub>2</sub>. Samples were then kept at -70°C before analysis by LC-MS/MS. Blood samples were thawed at room temperature. 10 µl of internal standard (tenovin-4, 5 ng in MeOH) was added to each tube and protein precipitation was carried out using five times the sample volume of acetonitrile. Samples were vortex mixed and centrifuged. The supernatant was then transferred directly into a HPLC vial for analysis. A standard curve for tenovin-1 was constructed for quantifying tenovin blood levels by spiking blank blood samples with known amounts of each tenovin (5 – 5000 ng/ml), followed by protein precipitation as outlined above for the test samples. Each concentration was made up in triplicate. LC-MS/MS was carried out using a Waters 2795 HPLC coupled to a Quattro Micro mass spectrometry system (MicroMass, UK) in the positive electrospray ionisation (ESI) mode. Chromatography was performed using a Kromasil C<sub>18</sub> ODS (5 µm, 150 × 3.2 mm) column (Phenomenex, Torrance, CA, USA). An isocratic mobile phase consisted of 70% acetonitrile:ammonium acetate buffer (5 mM, pH 3.5) and a flow rate of 0.4 ml/min was used. MS-MS data were processed using the QuanLynx quantify option of MassLynx software, version 4.0, from Micromass. Pharmacokinetic parameters were calculated using the WinNonLin software, version 3.1. A simple non-compartmental model was used to calculate AUC<sub>blood</sub>, CL, t<sub>1/2</sub> and C<sub>max</sub>.

**Table S3.** Heterozygous diploid yeast strains showing tenovin-6 hypersensitivity

ORF Name	Gene name	Hypersensitivity Index <sup>a</sup>	Function <sup>b</sup>
YOR008C-A	YOR008C-A	1.90	Uncharacterized ORF; synthetic lethal with <i>BUB3</i>
YDR496C	<i>PUF6</i>	1.70	<i>Pumilio</i> homology domain mRNA binding protein; polarized mRNA localization
YDL041W	Overlaps <i>SIR2</i>	1.40	Sirtuin family NAD <sup>+</sup> -dependent histone deacetylase; lifespan regulation; <i>HML</i> , <i>HMR</i> , telomere and rDNA silencing; negatively regulates initiation of DNA replication
YER166W	<i>DNF1</i>	1.36	Aminophospholipid translocase (flippase) with primarily plasma membrane localization; involved in endocytosis, protein transport and cell polarity
YJR103W	<i>URA8</i>	1.36	Minor CTP synthase isozyme
YLR005W	<i>SSL1</i>	1.35	Component of TFIIH, which is essential for transcription and nucleotide excision repair
YDL105W	<i>NSE4</i>	1.35	Nuclear protein; plays a role in the function of the Smc5p-Rhc18p complex
YGL103W	<i>RPL28</i>	1.33	Ribosomal protein L29
YNL328C	<i>MDJ2</i>	1.30	Constituent of the mitochondrial import motor associated with the presequence translocase
YDL128W	<i>VCX1</i>	1.28	Vacuolar H <sup>+</sup> /Ca <sup>2+</sup> exchanger; Ca <sup>2+</sup> homeostasis
YDL070W	<i>BDF2</i>	1.28	TFIID-associated protein; involved in transcription initiation at TATA-containing promoters
YBR245C	<i>ISW1</i>	1.27	ATP-dependent chromatin remodeller
YNL170W	Overlaps <i>PSD1</i>	1.27	Phosphatidylserine decarboxylase of the mitochondrial inner membrane
YDR363W	<i>ESC2</i>	1.25	Mating-type locus silencing; Sir2p interacting protein; may recruit or stabilize Sir proteins
YMR301C	<i>ATM1</i>	1.25	Mitochondrial inner membrane transporter; Fe/S cluster precursor export to the cytosol; member of the ABC transporter family
YGL228W	<i>SHE10</i>	1.25	Putative glycosylphosphatidylinositol (GPI)-anchored protein; unknown function

<sup>a</sup> Higher values indicate greater hypersensitivity; see text for details. <sup>b</sup> Functional annotations are derived from the *Saccharomyces* genome database (<http://www.yeastgenome.org>).

## Supplemental References

- Aronov, S., Gelin-Licht, R., Zipor, G., Haim, L., Safran, E., and Gerst, J. E. (2007). mRNAs encoding polarity and exocytosis factors are cotransported with the cortical endoplasmic reticulum to the incipient bud in *Saccharomyces cerevisiae*. *Mol Cell Biol* 27, 3441-3455.
- Berkson, R. G., Hollick, J. J., Westwood, N. J., Woods, J. A., Lane, D. P., and Lain, S. (2005). Pilot screening programme for small molecule activators of p53. *Int J Cancer* 115, 701-710.
- Brachmann, C. B., Sherman, J. M., Devine, S. E., Cameron, E. E., Pillus, L., and Boeke, J. D. (1995). The SIR2 gene family, conserved from bacteria to humans, functions in silencing, cell cycle progression, and chromosome stability. *Genes Dev* 9, 2888-2902.
- Daniel, J. A., Keyes, B. E., Ng, Y. P., Freeman, C. O., and Burke, D. J. (2006). Diverse functions of spindle assembly checkpoint genes in *Saccharomyces cerevisiae*. *Genetics* 172, 53-65.
- Ford, J., Jiang, M., and Milner, J. (2005). Cancer-specific functions of SIRT1 enable human epithelial cancer cell growth and survival. *Cancer Res* 65, 10457-10463.
- Gu, W., Deng, Y., Zenklusen, D., and Singer, R. H. (2004). A new yeast PUF family protein, Puf6p, represses ASH1 mRNA translation and is required for its localization. *Genes Dev* 18, 1452-1465.
- Linke, S. P., Clarkin, K. C., Di Leonardo, A., Tsou, A., and Wahl, G. M. (1996). A reversible, p53-dependent G0/G1 cell cycle arrest induced by ribonucleotide depletion in the absence of detectable DNA damage. *Genes Dev* 10, 934-947.
- Luo, J., Nikolaev, A. Y., Imai, S., Chen, D., Su, F., Shiloh, A., Guarente, L., and Gu, W. (2001). Negative control of p53 by Sir2alpha promotes cell survival under stress. *Cell* 107, 137-148.
- Pass, G. J., Carrie, D., Boylan, M., Lorimore, S., Wright, E., Houston, B., Henderson, C. J., and Wolf, C. R. (2005). Role of hepatic cytochrome p450s in the pharmacokinetics and toxicity of cyclophosphamide: studies with the hepatic cytochrome p450 reductase null mouse. *Cancer Res* 65, 4211-4217.
- Smart, P., Lane, E. B., Lane, D. P., Midgley, C., Vojtesek, B., and Lain, S. (1999). Effects on normal fibroblasts and neuroblastoma cells of the activation of the p53 response by the nuclear export inhibitor leptomycin B. *Oncogene* 18, 7378-7386.
- Vander Heiden, M. G., Choy, J. S., VanderWeele, D. J., Brace, J. L., Harris, M. H., Bauer, D. E., Prange, B., Kron, S. J., Thompson, C. B., and Rudin, C. M. (2002). Bcl-x(L) complements *Saccharomyces cerevisiae* genes that facilitate the switch from glycolytic to oxidative metabolism. *J Biol Chem* 277, 44870-44876.
- Vaziri, H., Dessain, S. K., Ng Eaton, E., Imai, S. I., Frye, R. A., Pandita, T. K., Guarente, L., and Weinberg, R. A. (2001). hSIR2(SIRT1) functions as an NAD-dependent p53 deacetylase. *Cell* 107, 149-159.